

# Adaptive Kalman Filters for Orbit Estimation of Navigation Satellites for DGPS Applications

*Dr. Ranjan Vepa, Mr. Amzari Zhahir*  
Queen Mary, University of London, London E1 4NS  
E-Mail: r.vepa@qmul.ac.uk

**Abstract** – The navigation problem associated with terminal aircraft guidance refers to position determination of an individual vehicle with respect to some point local to the environment as is the case with aircraft landing systems. This paper presents results for a relative navigation filter that achieves CAT3-level precision from a customized navigation satellite receiver's data message and the NORAD SDP4/SDP8 algorithm to establish the measured data. This work uses a precise, robust Unscented Kalman Filter (UKF) that is based on a realistic measurement model and a nonlinear propagation model. The UKF is based on the Unscented Transformation (UT) and provides a derivative free alternative to Extended Kalman filtering (EKF). Preliminary results indicate the method is particularly suitable for estimating the orbit ephemeris of navigation satellites such as GPS, Galileo and GLONASS. These estimates serve to generate pseudo-range corrections in an interoperable differential GNSS application.

## 1. Introduction

Differential Global Position System (DGPS) is a mode of operation of the Global Positioning System (GPS) satellite based positioning system that employs a reference station at a known location to calculate and broadcast corrections that could be applied to the pseudo-range by users in the vicinity of the receiver station. This approach is known to increase positional accuracy. In the literature, several algorithms have been developed that are designed to remove the effects of the so called common mode errors in all receivers in the vicinity of the reference station. These algorithms are based on the concepts of optimal filtering, in general and

on the EKF in particular, developed along the lines suggested by Farrell and Givargis [1] and Farrell et. al. [2].

Recent developments in differential GPS (DGPS) services have focussed mainly on employing a number of permanent reference stations to cover a certain area of operation. An alternative concept is based on the virtual reference station (VRS) concept. In this case, observation data for a non-existing "virtual" station are generated at a main or central reference station and transmitted to the virtual stations. This leads to a significant improvement in positioning accuracy. In the single reference station concept, a reference station in a DGPS network consists of the following main components: a GPS antenna/receiver assembly; a wireless data communication link to the user (usually a radio link); the reference station software on a PC which performs station monitoring, DGPS data correction model estimation and data archiving; interfaces and communication links for data transfer to the user. For integrity monitoring, a reference station usually consists of 2 independent GPS receivers to guarantee against system failure. The user receives either DGPS corrections for code positioning or real-time kinematic (RTK) data for carrier phase positioning in Radio Technical Commission for Maritime Services format. In the multiple station concept, multiple reference stations are connected to a central station using a data communication link such a LAN connection. Additional equipment at the reference station includes modems for data transfer and modification of the station software packages. The standard data transfer protocol is employed between each reference station and the control centre. The DGPS positioning accuracy at user's

position can be corrected by employing the pseudo-range correction information provided by the central and virtual reference stations. Thus the unknown user's position can be precisely calculated from the pseudo-range correction data.

Multi-station Differential GPS systems fall into one of three categories: measurement domain, position domain, and state-space domain as described by Abousalem [3]. Measurement domain algorithms provide the user with corrections from a reference station or a weighted average of corrections from a network of reference stations. In the position domain approach, the user computes independent positions using corrections from separate reference stations. A weighted average of these solutions is then computed. The disadvantage of both the measurement and position domain algorithms is a degradation of accuracy with distance from the network's centre. In contrast, the state-space approach models and estimates real physical parameters including satellite clocks and orbits, reference station troposphere and clocks. The ionosphere delays can additionally be modeled from dual-frequency reference station data for single-frequency end users. However for local area applications, such as aircraft landing the position domain approach may be the best suited.

In an aircraft landing system, not only does the pilot need to know his accurate position but also the reference station which needs a preliminary estimate of his position. In this case, the IDGPS (Inverted DGPS) would be more suitable than DGPS. In IDGPS, a vehicle sends its GPS position information, usually in NMEA format, to the reference station and the differential correction is made at the reference station, not at the GPS receiver in the vehicle. However, in contrast to a standard IGPS system, that does not require an RTCM transmission to the vehicle, the pilot requires an update on his position from the reference station. Thus this situation can be handled provided the aircraft itself is

treated as a roving virtual reference centre. The objective in using multiple reference stations in a network for GPS corrections is to model and correct for distance-dependent errors that reduce the accuracy of conventional RTK or DGPS positions in proportion to the distance from a rover to its nearest reference station. It is well known that the most significant sources of error affecting precise GPS positioning are the ionosphere, troposphere and satellite orbits. The influence of the ionospheric error on different frequencies in the L-band used by satellite navigation systems is well understood. The ionosphere, which is subject to rapid and localised disturbances, is the main restriction on the station density in a reference network. The troposphere and orbit errors have an equal effect on all ranging signals used by current satellite-based global navigation systems. The aim of a reference network is to model and estimate these error sources and provide this network correction information to the roving vehicle so that they may derive positions with a higher accuracy than with conventional RTK.

In an earlier paper, Vepa and Zhahir [4] discussed the development of two and three frequency reference station algorithms that may be employed with any navigation satellite. The motivation behind the design of the algorithms has been the need for reference station algorithms that can deal with an interoperable system of navigation satellites to obtain high accuracy positioning information local to the roving vehicle. In order to achieve interoperability we provided for additional satellite orbit corrections that will ensure the consistency of satellite orbit predictions. To account for the fact we are now dealing with a variety of satellites, we made no assumptions of the error covariance matrices and adopted an adaptive filter based on the Method of Maximum Likelihood Estimation (MMLE), a technique applied to the EKF by Mehra [5]. However corrections of the orbiting satellite's ephemeris are assumed to be independent of the other common mode errors and were not considered there.

In this paper we consider the issue of corrections to the orbiting satellites ephemeris. One of the major requirements that must be met in order to establish generic interoperable systems is to employ independent and yet consistent error models to ensure that the ephemerides employed by the different systems can be easily converted from one to the other. In fact there is need to use a standard ephemeris to identify a satellite in an orbit. Currently different satellite navigation systems, such as GPS, GLONASS and GNSS (Galileo) use different methods for orbit estimation, correction and prediction. Moreover the error dynamics models used are extremely complex (see for example Hoots et. al. [6]). Thus our aim is to develop a orbit prediction method that bears a direct straight forward relationship to the various methods currently in use. To this end we explored the application of various adaptive Kalman filters, including the UKF to the orbit estimation problem. Although the standard UKF was initially a promising alternative features of the orbital dynamics led us to believe that the standard UKF must be employed with appropriate restrictions on the noise covariance statistics, to facilitate the calculation of the sigma points. To address some of the shortcomings of the standard UKF we propose a modified approach to the UKF. The proposed modified UKF uses singular value decomposition rather than Cholesky decomposition to estimate the sigma points. Moreover the singular values are replaced by their absolute values in the decomposition. Thus we present the results of the application of the modified approach to the UKF to orbit estimation to demonstrate its superiority over the standard approach.

## 2. Adaptive Kalman Filters

The discrete Kalman filter, outlined by Brown and Huang [7], is the basis for developing the adaptive Kalman filter algorithm. Consider a linear discrete time model representing the error correction

states of for a generic differential satellite navigation system given by,

$$\mathbf{x}_k = \Phi_{k-1} \mathbf{x}_{k-1} + \mathbf{w}_{k-1} \quad (1a)$$

$$\mathbf{z}_k = \mathbf{H}_k \mathbf{x}_k + \mathbf{v}_k, \quad (1b)$$

where  $\mathbf{x}_k$  is a  $(n \times 1)$  state vector,  $\Phi_k$  is a  $(n \times n)$  transition matrix,  $\mathbf{z}_k$  is a  $(m \times 1)$  measurement vector and  $\mathbf{H}_k$  is a  $(m \times n)$  state to measurement distribution matrix. Variables  $\mathbf{w}_k$  and  $\mathbf{v}_k$  are uncorrelated Gaussian White noise sequences with zero means

$$E\{\mathbf{w}_k\} = E\{\mathbf{v}_k\} = 0 \quad (2)$$

and covariance matrices defined by:

$$E\{\mathbf{w}_k \mathbf{v}_i^T\} = 0 \text{ and } E\{\mathbf{w}_k \mathbf{w}_i^T\} = 0, \quad (3a)$$

$$E\{\mathbf{v}_k \mathbf{v}_i^T\} = 0 \text{ for } i \neq k, \quad (3b)$$

and

$$E\{\mathbf{w}_k \mathbf{w}_k^T\} = \mathbf{Q}_k, \quad E\{\mathbf{v}_k \mathbf{v}_k^T\} = \mathbf{R}_k \quad (3c)$$

where  $E\{\cdot\}$  is the expectation operator. The parameters,  $\mathbf{Q}_k$  and  $\mathbf{R}_k$  are the covariance matrices of the process noise sequence,  $\mathbf{w}_k$  and the measurement noise sequence,  $\mathbf{v}_k$  respectively.

The state and covariance prediction equations defining the Kalman filter (KF) are:

$$\hat{\mathbf{x}}_k^- = \Phi_{k-1} \hat{\mathbf{x}}_{k-1} \quad (4a)$$

$$\hat{\mathbf{P}}_k^- = \Phi_{k-1} \mathbf{P}_{k-1} \Phi_{k-1}^T + \mathbf{Q}_{k-1} \quad (4b)$$

where  $\hat{\mathbf{x}}_k^-$  is the state vector predicted from the corrected state vector,  $\hat{\mathbf{x}}_{k-1}$  estimated at the end of the previous epoch,  $\hat{\mathbf{P}}_k^-$  is the corresponding predicted state covariance matrix and  $\mathbf{P}_{k-1}$  is the corresponding predicted state covariance matrix at the end of the previous epoch. The measurement correction or update equations defining the KF are,

$$\mathbf{K}_k = \hat{\mathbf{P}}_k^- \mathbf{H}_k^T (\mathbf{H}_k \hat{\mathbf{P}}_k^- \mathbf{H}_k^T + \mathbf{R}_k)^{-1} \quad (5a)$$

$$\hat{\mathbf{x}}_k = \hat{\mathbf{x}}_k^- + \mathbf{K}_k (\mathbf{z}_k - \mathbf{H}_k \hat{\mathbf{x}}_k^-) \quad (5b)$$

$$\hat{\mathbf{P}}_k = (\mathbf{I} - \mathbf{K}_k \mathbf{H}_k) \hat{\mathbf{P}}_k^- \quad (5c)$$

where  $\mathbf{K}_k$  is the optimal Kalman gain, which defines the correction that must be added to the predicted state vector in order to obtain the estimate. The correction is a function of the innovation sequence which is,

$$\mathbf{v}_k = (\mathbf{z}_k - \mathbf{H}_k \hat{\mathbf{x}}_k^-). \quad (6)$$

The innovation sequence is a White Gaussian noise sequence with zero mean when the filter is optimal. Moreover the observation error and state estimation error are orthogonal to each other. The innovation sequence is different from the residual which is defined as,

$$\mathbf{r}_k = (\mathbf{z}_k - \mathbf{H}_k \hat{\mathbf{x}}_k) = \mathbf{v}_k + \mathbf{H}_k (\mathbf{x}_k - \hat{\mathbf{x}}_k). \quad (7)$$

Thus employing equation 7 one could express the measurement noise  $\mathbf{v}_k$  as a linear combination of two independent components, the residual,  $\mathbf{r}_k$  and the optimal error in the estimate.

Eliminating the measurements the innovation sequence may be expressed as,

$$\mathbf{v}_k = \mathbf{H}_k (\mathbf{x}_k - \hat{\mathbf{x}}_k^-) + \mathbf{v}_k \quad (8)$$

and the covariance of the innovation is,

$$E\{\mathbf{v}_k \mathbf{v}_k^T\} = \mathbf{H}_k \hat{\mathbf{P}}_k^- \mathbf{H}_k^T + \mathbf{R}_k. \quad (9)$$

Assuming that the models are linear but with predicted states and measurements corrupted by some additive Gaussian noise with known variance of the type described equations 1, then it is known that the KF converges to the steady state regardless of the initial conditions. The adaptive KF therefore assumes that the magnitudes of the covariance matrices of the additive Gaussian noises are unknown and seeks to estimate the noise covariance matrices  $\mathbf{Q}_k$  and  $\mathbf{R}_k$  pertaining respectively to the process and the measurement noise models. The adaptive KF is thus a method of self-tuning for adapting the covariance matrices,  $\mathbf{Q}_k$  and  $\mathbf{R}_k$  of the process and measurement noise model sequences. It is achieved by making the statistics of the KF innovation sequences consistent with their theoretical co-variances. This principle was established by Mehra [8] and can be employed to tune both  $\mathbf{Q}_k$  and  $\mathbf{R}_k$ . An estimate of the covariance of the innovation is obtained by averaging the previous innovation sequence over a window length  $N$ :

$$\mathbf{C}_v^{k,N} = \frac{1}{N} \sum_{j=k-N+1}^k \mathbf{v}_j \mathbf{v}_j^T \quad (10)$$

and the covariance of the measurement noise sequence may be updated in principle by employing the relation,

$$\hat{\mathbf{R}}_k = \mathbf{C}_v^{k,N} - \mathbf{H}_k \hat{\mathbf{P}}_k^- \mathbf{H}_k^T. \quad (11)$$

Assuming a fixed window length, the covariance matrix may be recursively updated by employing the recursive relation,

$$\mathbf{C}_v^{k+1,N} = \mathbf{C}_v^{k,N} + \frac{(\mathbf{v}_{k+1} \mathbf{v}_{k+1}^T - \mathbf{v}_{k-N+1} \mathbf{v}_{k-N+1}^T)}{N}. \quad (12)$$

One could also directly estimate  $\mathbf{R}_k$  from the measurement residual. In this case it has been shown by Mohamed and Schwarz [9] that one has,

$$\hat{\mathbf{R}}_k = \mathbf{C}_r^{k,N} + \mathbf{H}_k \hat{\mathbf{P}}_k \mathbf{H}_k^T \quad (13)$$

where,

$$\mathbf{C}_r^{k,N} = \frac{1}{N} \sum_{j=k-N+1}^k \mathbf{r}_j \mathbf{r}_j^T. \quad (14)$$

The covariance of the process noise satisfies the equation,

$$\begin{aligned} \mathbf{Q}_{k-1} &= \hat{\mathbf{P}}_k^- - \Phi_{k-1} \mathbf{P}_{k-1} \Phi_{k-1}^T \\ &= \mathbf{K}_k \mathbf{H}_k \hat{\mathbf{P}}_k^- + \hat{\mathbf{P}}_k - \Phi_{k-1} \mathbf{P}_{k-1} \Phi_{k-1}^T. \end{aligned} \quad (15)$$

Recognising that the state estimate is an optimal estimate and considering the covariance of the state correction,

$$\begin{aligned} \mathbf{C}_{\Delta \mathbf{x}}^{k,N} &= \frac{1}{N} \sum_{j=k-N+1}^k (\hat{\mathbf{x}}_k - \hat{\mathbf{x}}_k^-) (\hat{\mathbf{x}}_k - \hat{\mathbf{x}}_k^-)^T \\ &= \frac{1}{N} \sum_{j=k-N+1}^k \Delta \mathbf{x} \Delta \mathbf{x}^T, \end{aligned} \quad (16)$$

where,

$$\Delta \mathbf{x} = (\hat{\mathbf{x}}_k - \hat{\mathbf{x}}_k^-) - (\mathbf{x}_k - \hat{\mathbf{x}}_k), \quad (17)$$

it may be expressed as,

$$\mathbf{C}_{\Delta \mathbf{x}}^{k,N} = \frac{1}{N} \sum_{j=k-N+1}^k \Delta \mathbf{x} \Delta \mathbf{x}^T \approx \hat{\mathbf{P}}_k^- - \hat{\mathbf{P}}_k = \mathbf{K}_k \mathbf{H}_k \hat{\mathbf{P}}_k^-. \quad (18)$$

The covariance of the state correction, which is linearly related to the innovation may also be expressed as,

$$\mathbf{C}_{\Delta \mathbf{x}}^{k,N} = \frac{1}{N} \sum_{j=k-N+1}^k \Delta \mathbf{x} \Delta \mathbf{x}^T \approx \mathbf{K}_k \mathbf{C}_v^{k,N} \mathbf{K}_k^T. \quad (19)$$

This relationship between the covariance matrices suggests that the update of  $\mathbf{R}_k$  could be done by employing the covariance of the residual while the update of  $\mathbf{Q}_k$  could be done by employing the covariance of the state correction. Hence the equation for

updating the covariance of the process noise may be expressed in principle as,

$$\mathbf{Q}_{k-1} = \hat{\mathbf{Q}}_{k-1} \equiv \mathbf{C}_{\Delta x}^{k,N} + \hat{\mathbf{P}}_k - \Phi_{k-1} \mathbf{P}_{k-1} \Phi_{k-1}^T. \quad (20a)$$

In some references (see for example Myers and Tapley [10], Blanchet, Frankignoul and Cane [11]) an unbiased estimator is employed for the covariance of the state correction and equation 20a is expressed as,

$$\mathbf{Q}_{k-1} = \frac{N}{N-1} \mathbf{C}_{\Delta x}^{k,N} + \hat{\mathbf{P}}_k - \Phi_{k-1} \mathbf{P}_{k-1} \Phi_{k-1}^T. \quad (20b)$$

### 3. The Extended and Unscented Kalman Filters

Most dynamic models employed for purposes of estimation or filtering of pseudo range errors or orbit ephemeris errors are generally not linear. To extend and overcome the limitations of linear models, a number of approaches such as the EKF have been proposed in the literature for nonlinear estimation using a variety of approaches. Unlike the KF, the EKF may diverge, if the consecutive linearizations are not a good approximation of the linear model over the entire uncertainty domain. Yet the EKF provides a simple and practical approach to dealing with essential non-linear dynamics. The model takes the form,

$$\mathbf{x}_k = \mathbf{f}_{k-1}(\mathbf{x}_{k-1}) + \mathbf{w}_{k-1} \quad (21)$$

$$\mathbf{z}_k = \mathbf{h}_k(\mathbf{x}_k) + \mathbf{v}_k. \quad (22)$$

Given the Jacobians,

$$\Phi_{k-1} = \nabla \mathbf{f}_{k-1}(\hat{\mathbf{x}}_{k-1}), \quad (23)$$

and

$$\mathbf{H}_k = \nabla \mathbf{h}_k(\hat{\mathbf{x}}_k^-), \quad (24)$$

the state prediction equation defining the EKF is:

$$\hat{\mathbf{x}}_k^- = \mathbf{f}_{k-1}(\hat{\mathbf{x}}_{k-1}) \quad (25)$$

while the covariance prediction equation is,

$$\hat{\mathbf{P}}_k^- = \Phi_{k-1} \mathbf{P}_{k-1} \Phi_{k-1}^T + \mathbf{Q}_{k-1}. \quad (26)$$

The measurement correction equations defining the EKF are,

$$\mathbf{K}_k = \hat{\mathbf{P}}_k^- \mathbf{H}_k^T (\mathbf{H}_k \hat{\mathbf{P}}_k^- \mathbf{H}_k^T + \mathbf{R}_k)^{-1} \quad (27)$$

$$\hat{\mathbf{x}}_k = \hat{\mathbf{x}}_k^- + \mathbf{K}_k [\mathbf{z}_k - \mathbf{h}_k(\hat{\mathbf{x}}_k^-)] \quad (28)$$

$$\hat{\mathbf{P}}_k = (\mathbf{I} - \mathbf{K}_k \mathbf{H}_k) \hat{\mathbf{P}}_k^-. \quad (29)$$

Equations 26, 27 and 29 are identical to equations 4b, 5a and 5c respectively. The

main difficulty in applying the algorithm to problems related to the estimation of orbital ephemeris is in determining the proper Jacobian matrices. The UKF is a feasible alternative that has been proposed to overcome this difficulty, by Julier and Uhlman [12] an effective way of applying the KF to nonlinear systems.

The UKF gets its name from the Unscented transformation, which is a method of calculating the mean and covariance of a random variable undergoing nonlinear transformation  $\mathbf{y} = \mathbf{f}(\mathbf{w})$ . Although it is a derivative free approach, it does not really address the divergence problem. In essence the method constructs a set of *sigma vectors* and propagates them through the same non-linear function. The mean and covariance of the transformed vector are approximated as a weighted sum of the transformed *sigma vectors* and their covariance matrices.

Consider a random variable  $\mathbf{w}$  with dimension  $L$  which is going through the nonlinear transformation,  $\mathbf{y} = \mathbf{f}(\mathbf{w})$ . The initial conditions are that  $\mathbf{w}$  has a mean  $\bar{\mathbf{w}}$  and a covariance  $\mathbf{P}_{ww}$ . To calculate the statistics of  $\mathbf{y}$ , a matrix  $\chi$  of  $2L + 1$  sigma vectors is formed. Sigma vector points are calculated according to the following conditions:

$$\chi_0 = \bar{\mathbf{w}} \quad (30a)$$

$$\chi_i = \bar{\mathbf{w}} + \left( \sqrt{(L + \lambda) \mathbf{P}_{ww}} \right)_i, \quad i = 1, 2, \dots, L, \quad (30b)$$

$$\chi_i = \bar{\mathbf{w}} - \left( \sqrt{(L + \lambda) \mathbf{P}_{ww}} \right)_i, \quad i = L+1, L+2, \dots, 2L, \quad (30c)$$

where,

$$\lambda = \alpha^2 (L + \kappa) - L,$$

$\alpha$  is a scaling parameter between 0 and 1 and  $\kappa$  is a secondary scaling parameter.

$\left( \sqrt{(L + \lambda) \mathbf{P}_{ww}} \right)_i$  is the  $i^{\text{th}}$  column of the matrix square root. This matrix square root can be obtained by Cholesky factorization. The weights associated with the sigma vectors are calculated from the following:

$$W_0^{(m)} = \lambda / (L + \lambda) \quad (31a)$$

$$W_0^{(c)} = (\lambda / (L + \lambda)) + 1 - \alpha^2 + \beta \quad (31b)$$

$$W_i^{(m)} = W_i^{(c)} = 1/2(L + \lambda),$$

$$i = 1, 2, \dots, 2L, \quad (31c)$$

where  $\beta$  is chosen as 2 for Gaussian distributed variables. The mean, covariance and cross-covariance of  $\mathbf{y}$  calculated using the UT are given by,

$$\mathbf{f}_i = \mathbf{f}(\boldsymbol{\chi}_i) \quad (32a)$$

$$\bar{\mathbf{y}} \approx \sum_{i=0}^{2L} W_i^{(m)} \mathbf{y}_i \quad (32b)$$

$$\mathbf{P}_{yy} \approx \sum_{i=0}^{2L} W_i^{(c)} (\mathbf{y}_i - \bar{\mathbf{y}})(\mathbf{y}_i - \bar{\mathbf{y}})^T \quad (32c)$$

$$\mathbf{P}_{xy} \approx \sum_{i=0}^{2L} W_i^{(c)} (\boldsymbol{\chi}_i - \bar{\boldsymbol{\chi}})(\mathbf{y}_i - \bar{\mathbf{y}})^T \quad (32d)$$

where  $W_i^{(m)}$  and  $W_i^{(c)}$  are the set of weights defined in a manner so approximations of the mean and covariance are accurate up to third order for Gaussian inputs for all nonlinearities, and to at least second order for non-Gaussian inputs. The sigma points in the sigma vectors are updated using the nonlinear model equations without any linearisation.

Given a general discrete nonlinear dynamic system in the form,

$$\mathbf{x}_{k+1} = \mathbf{f}(\mathbf{x}_k, \mathbf{u}_k) + \mathbf{w}_k, \quad \mathbf{y}_k = \mathbf{h}(\mathbf{x}_k) + \mathbf{v}_k \quad (33)$$

where  $\mathbf{x}_k \in R^n$  is the state vector,  $\mathbf{u}_k \in R^r$  is the known input vector,  $\mathbf{y}_k \in R^m$  is the output vector at time  $k$ .  $\mathbf{w}_k$  and  $\mathbf{v}_k$  are, respectively, the disturbance or process noise and sensor noise vectors, which are assumed to Gaussian white noise with zero mean. Furthermore  $\mathbf{Q}_k$  and  $\mathbf{R}_k$  are assumed to be the covariance matrices of the process noise sequence,  $\mathbf{w}_k$  and the measurement noise sequence,  $\mathbf{v}_k$  respectively. The UTs of the states are denoted as,

$$\mathbf{f}^{UT} = \mathbf{f}^{UT}(\mathbf{x}_k, \mathbf{u}_k), \quad \mathbf{h}^{UT} = \mathbf{h}^{UT}(\mathbf{x}_k) \quad (34)$$

while the transformed covariance matrices and cross-covariance are respectively denoted as,

$$\mathbf{P}_k^f = \mathbf{P}_k^f(\hat{\mathbf{x}}_k, \mathbf{u}_k), \quad \mathbf{P}_k^h = \mathbf{P}_k^h(\hat{\mathbf{x}}_k) \quad (35a)$$

and

$$\mathbf{P}_k^{fh} = \mathbf{P}_k^{fh}(\hat{\mathbf{x}}_k, \mathbf{u}_k). \quad (35b)$$

The UKF estimator can then be expressed in a compact form. The state time-update equation, the predicted covariance, the

Kalman gain the state estimate and the corrected covariance are respectively given by,

$$\hat{\mathbf{x}}_k^- = \mathbf{f}_{k-1}^{UT}(\hat{\mathbf{x}}_{k-1}) \quad (36a)$$

$$\hat{\mathbf{P}}_k^- = \mathbf{P}_{k-1}^f + \mathbf{Q}_{k-1} \quad (36b)$$

$$\mathbf{K}_k = \hat{\mathbf{P}}_k^{fh} (\hat{\mathbf{P}}_k^{h-} + \mathbf{R}_k)^{-1} \quad (36c)$$

$$\hat{\mathbf{x}}_k = \hat{\mathbf{x}}_k^- + \mathbf{K}_k [\mathbf{z}_k - \mathbf{h}_k^{UT}(\hat{\mathbf{x}}_k^-)] \quad (36d)$$

$$\hat{\mathbf{P}}_k = \hat{\mathbf{P}}_k^- - \mathbf{K}_k (\hat{\mathbf{P}}_k^{h-} + \mathbf{R}_k)^{-1} \mathbf{K}_k^T. \quad (36e)$$

Thus higher order non-linear models capturing significant aspects of the dynamics may be employed to ensure that the KF algorithm can be implemented to effectively estimate the states in practice.

For our purposes we adopt the both the UKF and EKF approaches to estimate orbit parameters using an adaptive approach. The methods of adapting the parameter matrices,  $\mathbf{Q}_k$  and  $\mathbf{R}_k$ , defined earlier for the case of the linear discrete model may be employed.

#### 4. Orbit Modelling

The most commonly employed model in navigation theory is based on the Lagrange planetary equations for the Keplerian orbital elements which is the basis for a variety of satellite error models (see for example Filipinski, M. N. and Varatharajoo, R. [13]). However these equations which are patently non-linear may not provide the best parameterisation of the orbit for purposes of orbit estimation. Orbital dynamics has been classically expressed in terms of Cartesian position and velocity coordinates in inertial and in rotating coordinate frames. In a rotating reference frame, a dynamic model for the acceleration is obtained by including the effects of normal central force field and the primary disturbance effect due to the Earth's equatorial bulge and flattening at the poles. The Earth's equatorial bulge and flattening at the poles is due to the Earth's oblateness and is represented by two coefficients,  $C_{2i}$ ,  $i = 0$  and 2.

A length scale and a time normalization defined by,

$$r_s = \left(\mu/\Omega_n^2\right)^{1/3}, \tau = \Omega_n t,$$

are introduced, where  $\Omega_n$  is the angular velocity of the rotating frame. The equations of motion are then expressed in terms of non-dimensional Cartesian coordinates,  $\tilde{x}$ ,  $\tilde{y}$ ,  $\tilde{z}$ , as:

$$d\tilde{x}/d\tau = \tilde{x}', \quad d\tilde{y}/d\tau = \tilde{y}', \quad d\tilde{z}/d\tau = \tilde{z}', \quad (37a)$$

$$\frac{d\tilde{x}'}{d\tau} = -\frac{\mu_n}{\tilde{r}^3} \tilde{x} + \mu_n \frac{\partial \tilde{U}_2}{\partial \tilde{x}} + \tilde{x} + 2\tilde{y}' + \tilde{x}''_{res}, \quad (37b)$$

$$\frac{d\tilde{y}'}{d\tau} = -\frac{\mu_n}{\tilde{r}^3} \tilde{y} + \mu_n \frac{\partial \tilde{U}_2}{\partial \tilde{y}} + \tilde{y} - 2\tilde{x}' + \tilde{y}''_{res}, \quad (37c)$$

$$\frac{d\tilde{z}'}{d\tau} = -\frac{\mu_n}{\tilde{r}^3} \tilde{z} + \mu_n \frac{\partial \tilde{U}_2}{\partial \tilde{z}} + \tilde{z}''_{res}, \quad (37d)$$

where,  $\mu_n = \mu/\Omega_n^2 r_s^3 = 1$ ,  $\tilde{r} = \sqrt{\tilde{x}^2 + \tilde{y}^2 + \tilde{z}^2}$ ,  $\mu$  is the gravity parameter, and  $\tilde{x}''_{res}$ ,  $\tilde{y}''_{res}$ ,  $\tilde{z}''_{res}$  are the residual accelerations mainly due to the gravitational effects of the Moon and Sun. These are generally modeled as sum of biases and periodic terms including second harmonics.

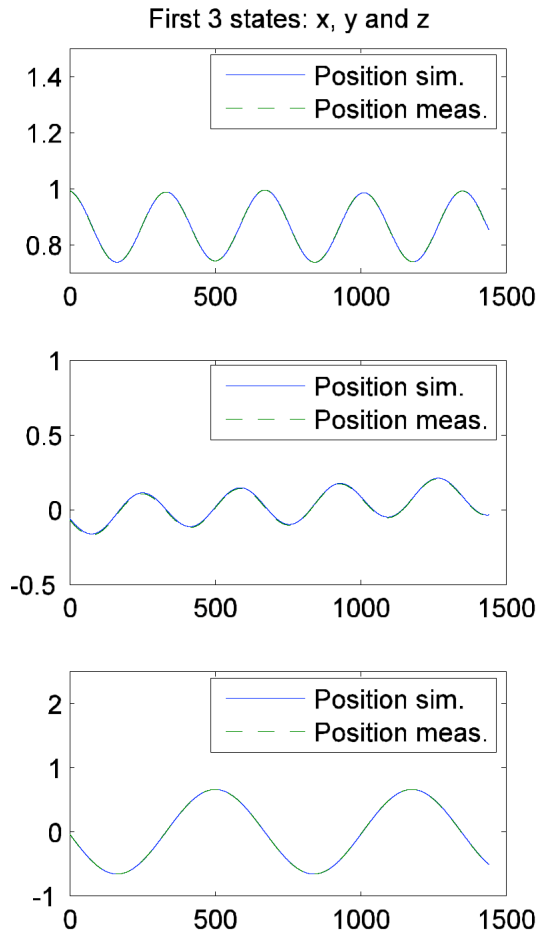


**Fig. 1a. GLONASS satellite position prediction normalised to orbit radius versus time in minutes.**

The Earth's gravitational perturbation potential can be expressed as,

$$U_2 = \frac{\mu C_{20}}{r^3} \left(1 - \frac{3}{2} \cos^2 \delta\right) + \frac{3\mu C_{22}}{r^3} \cos^2 \delta \cos 2\lambda$$

where  $r$  is the distance of the body centre of mass,  $\delta$  is the latitude measured from the equatorial plane, and  $\lambda$  is the longitude measured from the long end of the body (about  $15^\circ$  west longitude in the case of the Earth). In Earth fixed Cartesian coordinates, with the  $x$ - $y$  plane in the Earth's equatorial plane, the potential may be approximately expressed as,

$$U_2 = -\mu C_{20} \frac{(r^2 - 3z^2)}{2r^5} + 3\mu C_{22} \frac{(x^2 - y^2)}{r^5},$$

where  $r = \sqrt{x^2 + y^2 + z^2}$ .

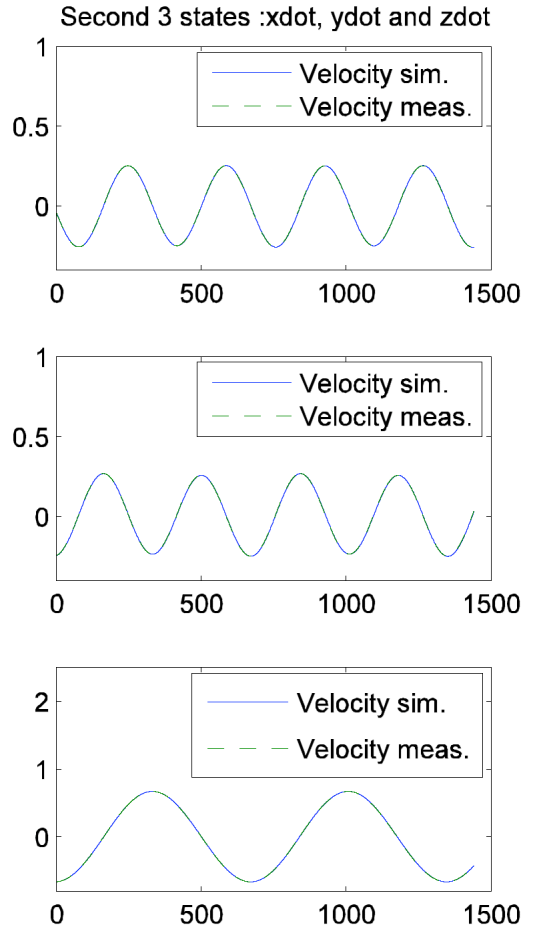


**Fig. 1b. GLONASS satellite normalised velocity prediction versus time in minutes.**

In terms of the normalised coordinates Earth fixed  $(\tilde{x}_e, \tilde{y}_e, \tilde{z}_e)$  and rotating  $(\tilde{x}, \tilde{y}, \tilde{z})$  coordinates, assuming that the reference  $x$ - $y$  plane is inclined to the Earth's equatorial plane by a fixed angle, the gradients of the non-dimension Earth's gravitational perturbation potential,  $\tilde{U}_2$ , in rotating coordinates are,

$$\begin{aligned} \frac{\partial \tilde{U}_2}{\partial \tilde{x}} = & -\frac{\tilde{C}_{20}}{\tilde{r}^5} \tilde{x} + \frac{5\tilde{C}_{20}\tilde{x}}{2\tilde{r}^7} (\tilde{r}^2 - 3\tilde{z}_e^2) \\ & + 3\frac{\tilde{C}_{20}\tilde{x}_e}{\tilde{r}^5} \sin i \cos \Omega_r \tau + \frac{6\tilde{C}_{22}}{\tilde{r}^5} \tilde{x} \\ & - \frac{15\tilde{C}_{22}\tilde{x}}{\tilde{r}^7} (\tilde{x}_e^2 - \tilde{y}_e^2), \end{aligned} \quad (38a)$$

$$\begin{aligned} \frac{\partial \tilde{U}_2}{\partial \tilde{y}} = & -\frac{\tilde{C}_{20}\tilde{y}}{\tilde{r}^5} + \frac{5\tilde{C}_{20}\tilde{y}}{2\tilde{r}^7} (\tilde{r}^2 - 3\tilde{z}_e^2) \\ & - 3\frac{\tilde{C}_{20}\tilde{x}_e}{\tilde{r}^5} \sin i \sin \Omega_r \tau + \frac{6\tilde{C}_{22}}{\tilde{r}^5} \tilde{y} \\ & - \frac{15\tilde{C}_{22}\tilde{y}}{\tilde{r}^7} (\tilde{x}_e^2 - \tilde{y}_e^2), \end{aligned} \quad (38b)$$

$$\begin{aligned} \frac{\partial \tilde{U}_2}{\partial \tilde{z}} = & -\frac{\tilde{C}_{20}\tilde{z}}{\tilde{r}^5} + 3\frac{\tilde{C}_{20}\tilde{z}_e}{\tilde{r}^5} \cos i \\ & + \frac{5\tilde{C}_{20}\tilde{z}}{2\tilde{r}^7} (\tilde{r}^2 - 3\tilde{z}_e^2) - \frac{6\tilde{C}_{22}}{\tilde{r}^5} \tilde{x}_e \sin i \\ & - \frac{15\tilde{C}_{22}\tilde{z}}{\tilde{r}^7} (\tilde{x}_e^2 - \tilde{y}_e^2), \end{aligned} \quad (38c)$$

where,

$$\begin{bmatrix} \tilde{x}_e \\ \tilde{y}_e \\ \tilde{z}_e \end{bmatrix} = \begin{bmatrix} \cos \Omega_r \tau & -\sin \Omega_r \tau & 0 \\ \sin \Omega_r \tau & \cos \Omega_r \tau & 0 \\ 0 & 0 & 1 \end{bmatrix} \begin{bmatrix} \tilde{x} \\ \tilde{y} \\ \tilde{z} \end{bmatrix} \equiv \mathbf{T}_\Omega \begin{bmatrix} \tilde{x} \\ \tilde{y} \\ \tilde{z} \end{bmatrix},$$

$$\begin{bmatrix} \tilde{x}_e \\ \tilde{y}_e \\ \tilde{z}_e \end{bmatrix} = \begin{bmatrix} \cos i & 0 & -\sin i \\ 0 & 1 & 0 \\ \sin i & 0 & \cos i \end{bmatrix} \begin{bmatrix} \tilde{x}_e \\ \tilde{y}_e \\ \tilde{z}_e \end{bmatrix} = \mathbf{T}_i \begin{bmatrix} \tilde{x}_e \\ \tilde{y}_e \\ \tilde{z}_e \end{bmatrix},$$

$$\tilde{x} = \tilde{x}_e \cos i \cos \Omega_r \tau + \tilde{y}_e \sin \Omega_r \tau,$$

$$\tilde{y} = -\tilde{x}_e \cos i \sin \Omega_r \tau + \tilde{y}_e \cos \Omega_r \tau,$$

$\Omega_r$  is the relative angular velocity of the satellite to the Earth fixed frame,  $i$  is the inclination orbit to the Earth's equatorial plane and  $\tilde{C}_{2i} = C_{2i}/r_s^2$ . The oblateness coefficients,  $C_{2i}$ , are also related to the principal moments of inertia of the Earth and could be expressed in terms of alternate relationships to the zonal harmonic coefficients,  $J_2 = 1.082616 \times 10^{-3}$ ,

$J_3 = -2.53881 \times 10^{-6}$ ,  $J_4 = -1.65597 \times 10^{-6}$  and to  $J_{21} = 0$ ,  $J_{22} = 1.86 \times 10^{-6}$ ,  $J_{31} = 2.1061 \times 10^{-6}$ . The orbit is defined by equations 37 and 38. These can be numerically integrated and compared with the position and velocity data for a typical GLONASS navigation satellite independently generated from the NORAD Two Line Element dataset from celestrak website[14] by using the SDP4 method, (Hoots et. al. [6]) with the position normalised to a mean altitude of 25490 km, and the velocity to the mean circular velocity of 3.9545 km/sec. These position and velocity responses are shown in figures 1 and 2 respectively.

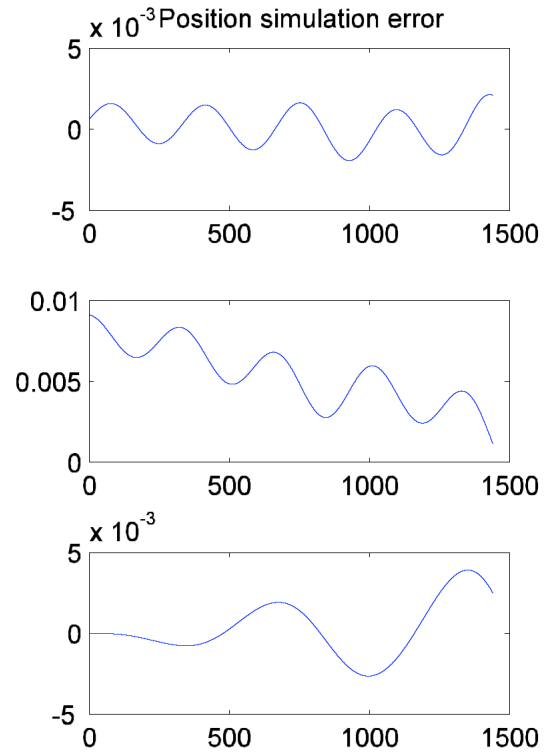
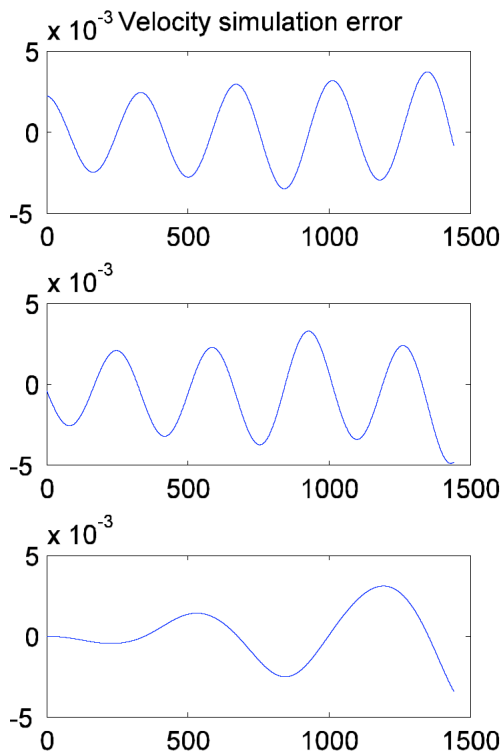


Fig. 2a. GLONASS satellite position prediction error versus time in minutes.

The results indicate that the simulated response follows the measured position and velocity data quite accurately. However looking very closely at the figures, one may observe that the simulated responses drift very slowly away from the measurements due to the presence of secular terms thus establishing the need for filtering. It is also observed that the simulation of the nonlinear dynamics correctly predicts the harmonic response

which is absent in the response obtained from the Hill-Clohessy-Wiltshire type linearised equations of motion.



**Fig. 2b. GLONASS satellite velocity prediction error versus time in minutes.**

### 5. UKF based Orbit Estimation

In the case of the classical linear KF which is not only an optimal filter but also an asymptotically stable filter, the filter estimates can be expected to follow the measurements closely even when the states of the process or plant model are unstable. However in the above orbit model it is not possible to apply the linear KF and, for this reason, we choose to employ the UKF. In figures 3 and 4 the state estimates for the position and velocity errors and the error in the measurement estimate are shown for the same satellite as in figures 1 and 2. The measurement vector consists of six independent simulations of the position and velocity as well actual measurements of the pseudo range. The maximum predicted error in the pseudo-range is thus less than 10m relative to the data generated for the GLONASS satellite. It is clear that the estimates tend to follow the states of the plant model and the

measured position and velocity data. Moreover the observed drift rates in the simulations are reduced. However there is need for some caution in applying the UKF due to its limitations.

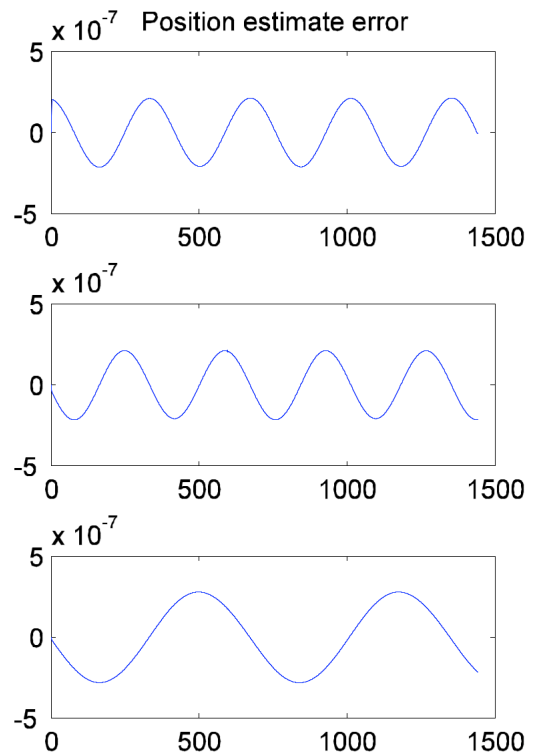


**Fig. 3a GLONASS satellite UKF based position estimate error versus time in minutes.**

The UKF is based on approximating the probability distribution function than to approximating a nonlinear function as in the case of EKF. The state distributions are approximated by a Gaussian probability density, which is represented by a set of deterministically chosen sample points. The nonlinear filtering using the Gaussian representation of the posterior probability density via a set of deterministically chosen sample points is the basis for the UKF. Thus it is based on statistical linearization of the state dynamics rather than analytical linearization (as in the EKF). The statistical linearization is performed by employing linear regression using a set of regression (sample) points. The mean and covariance at the sigma points represent the true mean and covariance of the Gaussian density. When transformed to the nonlinear systems, they represent the true mean and covariance accurately only to the second

order of the nonlinearity. Thus this can be a severe limitation of the UKF unless the nonlinearities are limited to the first and second order in the process model.

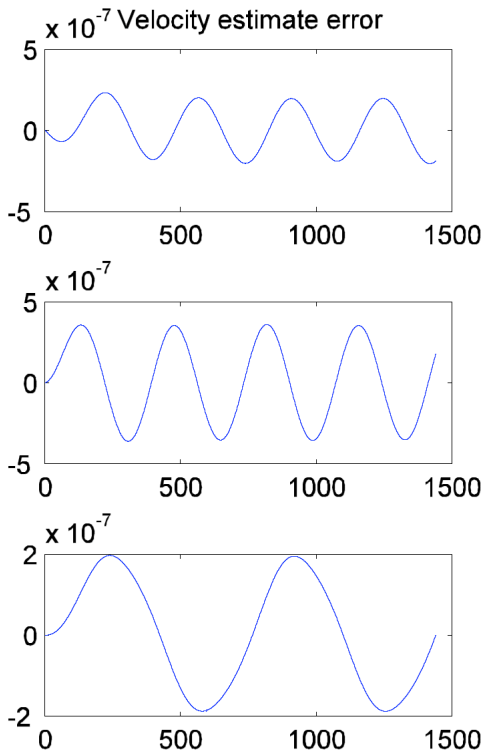


Fig. 3b GLONASS satellite UKF based velocity estimate error versus time in minutes.

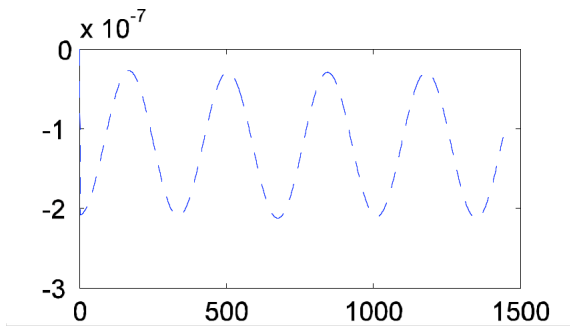


Fig. 4 GLONASS satellite UKF based pseudo-range estimate error versus time in minutes.

## 6. Modified UKF based Orbit Estimation

One of the difficulties that one encounters repeatedly while using the UKF algorithm is the fact the matrix  $\mathbf{P}_{ww}$  in equations 30a and 30b is not positive definite. Consequently one needs to choose  $\mathbf{Q}_k$  and  $\mathbf{R}_k$  in equations 36 to be sufficiently

positive definite so as to prevent  $\mathbf{P}_{ww}$  from becoming negative definite. This imposes an undue and unrealistic constraint on nature of the noise sequences which would no longer represent the true statistics of the process and sensor noise vectors.

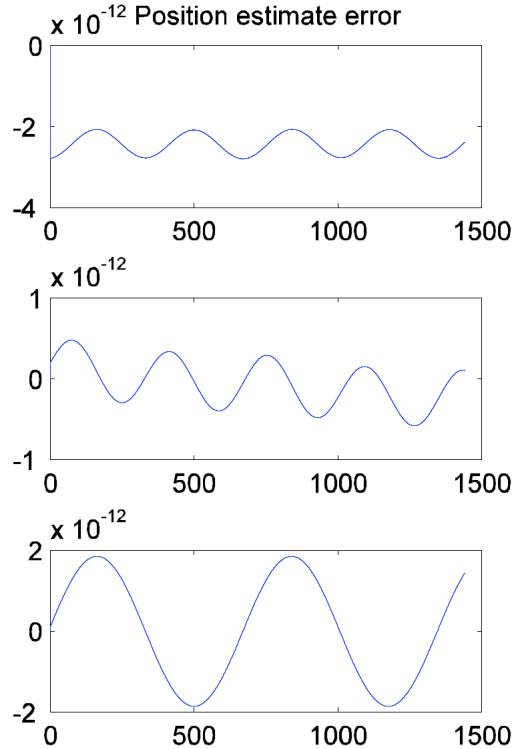
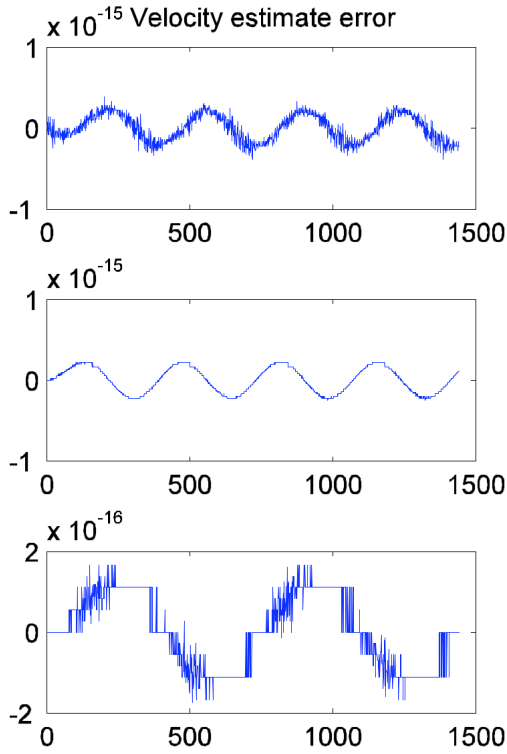


Fig. 5a GLONASS satellite modified UKF based position estimate error versus time in minutes.

To avoid this problem we do not employ the Cholesky decomposition method in computing the square root of  $\mathbf{P}_{ww}$  and employ the method of singular value decomposition (SVD) and then replace the singular values by their absolute values. This is a perfectly valid alternative in computing the sigma points and then there is no need to choose  $\mathbf{Q}_k$  and  $\mathbf{R}_k$  in equations 36 to be sufficiently positive definite so as to prevent  $\mathbf{P}_{ww}$  from becoming negative definite. This modification of the UKF algorithm resulted in a remarkable improvement in the performance of the UKF. In figures 5 and 6 the state estimates for the position and velocity errors and the error in the measurement estimate are shown for the same satellite as in figures 3 and 4, where

the estimates are now obtained by the modified UKF.



**Fig. 5b GLONASS satellite modified UKF based velocity estimate error versus time in minutes.**

The maximum predicted error in the pseudo-range is now reduced to less than 1mm relative to the data generated for the GLONASS satellite. Moreover it is clear that the estimated error is considerable more uniform in figure 6 than it is in figure 4, where it is quite visibly sinusoid and biased. Thus with the use of the proposed modification in place it is possible to substantially improve the performance of the UKF, because it facilitates the use of the most appropriate approximations for the noise statistics.

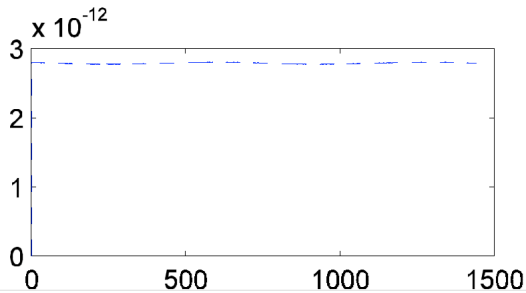


**Fig. 6 GLONASS satellite modified UKF based pseudo-range estimate error versus time in**

minutes.

We also observe from figure 6 that the magnitude of the measurement error is still biased. This is to be expected as we are only seeking to estimate the orbital errors which contribute exclusively to the errors in the satellite's ephemeris.

## 7. Adaptive UKF based Orbit Estimation

In order to employ the UKF when precise statistics of the process and measurement noise vectors are not available, the adaptive filter method proposed by Song, Qi and Han [15] is used to estimate the orbit parameters. The covariance matrixes of measurement residuals are recursively updated in the UKF.

The measurement and state noise covariance matrices, in the case of the UKF, may be expressed as:

$$\hat{\mathbf{R}}_k \equiv \mathbf{C}_v^{k,N} - \hat{\mathbf{P}}_k^{h-}, \quad (39a)$$

$$\hat{\mathbf{Q}}_{k-1} \equiv \mathbf{C}_{\Delta x}^{k,N} + \hat{\mathbf{P}}_k - \mathbf{P}_{k-1}^f \quad (39b)$$

which are analogous to equation 11 and the right hand side of equation 20. Corresponding equation 13 we may express the measurement noise covariance as,

$$\hat{\mathbf{R}}_k = \mathbf{C}_r^{k,N} + \hat{\mathbf{P}}_k^h \quad (40)$$

which involves the further computation of  $\hat{\mathbf{P}}_k^h$ , by applying the unscented nonlinear transformation,  $\mathbf{h}^{UT}(\hat{\mathbf{x}}_k)$  to the state estimate,  $\hat{\mathbf{x}}_k$ . The measurement noise covariance may be updated in principle by employing the equation 39a.

The nonlinear relationships between the covariance matrices also suggests that the update of  $\mathbf{R}_k$  could be done by employing the covariance of the residual (equation 40) while the update of  $\mathbf{Q}_k$  could be done by employing the covariance of the state correction (equation 39b). However the simultaneous adaptation of both  $\mathbf{Q}_k$  and  $\mathbf{R}_k$  is not considered robust, as discussed by Blanchet, Frankignoul and Cane [11]. For this reason we restrict our attention to  $\mathbf{Q}_k$  adaptation as it is the process statistics that is really unknown. Furthermore it was

observed that the magnitudes of the filter gains were relatively small and for this reason equation 39b was approximated as,

$$\hat{\mathbf{Q}}_{k-1} \approx \mathbf{C}_{\Delta x}^{k,N} \quad (41)$$

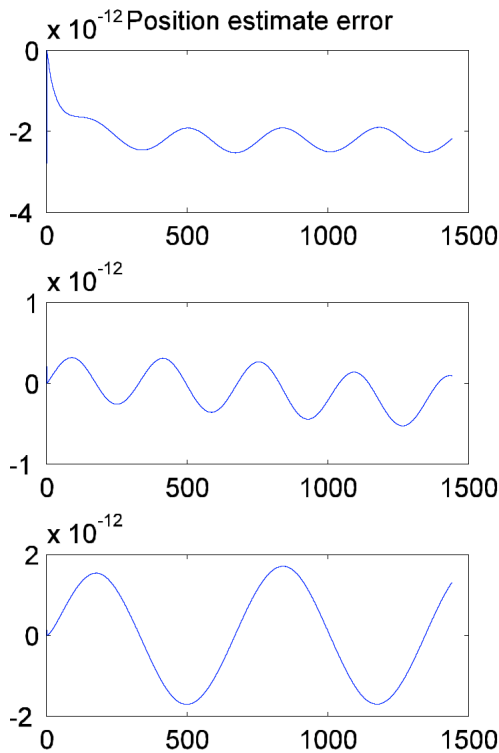


**Fig. 7a GLONASS satellite adaptive UKF based position estimate error versus time in minutes.**

The results of applying the adaptation scheme, with the additional modification in computing the square root of the covariance matrices by employing SVD as discussed in the preceding section, are illustrated in figures 7 and 8. These results clearly demonstrate the usefulness of the adaptive modified UKF.

The results indicated that the bias and drift in the estimate produced by the adaptive UKF, as it approaches steady state, are of the same order as the modified UKF. Moreover it takes at least an hour to approach steady state.

## 8. Conclusions and Discussion

The UKF is far better than the EKF over a relatively large time frame. It is observed that the UKF is tracking the true state over the entire time frame. Earlier experience

with the EKF indicates that it is unable to track the true state as the estimate tends to slowly drift from it. The main reason for the better performance of the UKF is that the UT approximates the mean and the covariance to third order which is better than linearization. Furthermore the modified UKF facilitates the use of arbitrary realistic models of the process and measurement noise statistics and thus gives a very good estimate of a navigation satellite's pseudo-range.

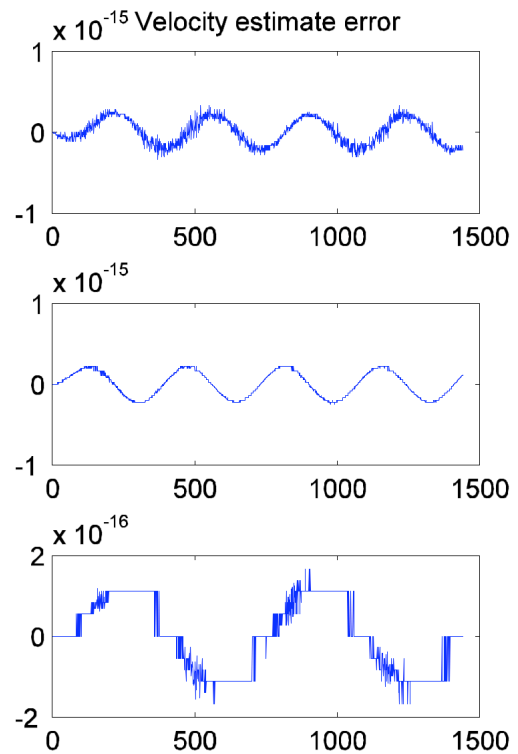


**Fig. 7b GLONASS satellite adaptive UKF based velocity estimate error versus time in minutes.**

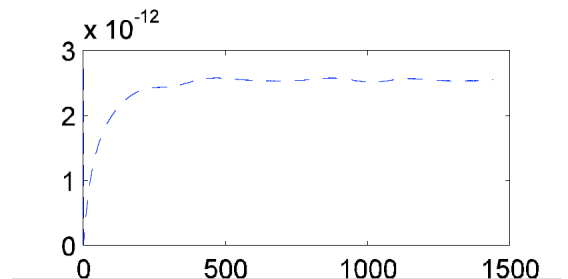


**Fig. 8 GLONASS satellite adaptive UKF based pseudo-range estimate error versus time in minutes.**

In most orbit predictions there is little *a priori* information about the state and measurement noise inputs. For this reason

adaptive filtering is appropriate as it allows for the interoperable operation of the orbit estimator as it permits one to switch from one satellite model to another. Thus the adaptive UKF serves to generate pseudo-range corrections in an interoperable differential GNSS application. Moreover the performance of the adaptive UKF is almost as accurate as the modified UKF.

## REFERENCES

1. Farrell, J., and Givargis, T., "Differential GPS Reference Station Algorithm—Design and Analysis," IEEE Transactions on Control Systems Technology, Vol. 8, No. 3, May 2000, 519-531.
2. Farrell, J., Givargis, T., & Barth, M., "Real-time differential carrier phase GPS-aided INS," IEEE Transactions on Control Systems Technology, Vol 8, No. 4, 2000, 709-721,
3. Abousalem, M., "Development and Analysis of Wide Area Differential GPS Algorithms," Ph.D. Dissertation, 1996, Department of Geomatics Engineering, The University of Calgary, Calgary, Alberta, Canada, 20083.
4. Vepa R. and Zhahir, A., Adaptive Extended Kalman Filter for DGPS and Carrier-phase DGPS Applications, Poster/paper presented at European Navigation Conference, ENC-GNSS-2008, held in Toulouse, France, 23-25 April, 2008.
5. Mehra, R. K., "On the Identification of Variances and Adaptive Kalman Filtering," IEEE Transactions on Automatic Control, Vol. AC-15, No. 2, April 1970, pp. 175-184.
6. Hoots, F. R., Schumacher Jr., P. W. and Glover, R. A., "History of Analytical Orbit Modelling in the U.S. Space Surveillance System," J. of Guidance, Control and Dynamics, Vol. 27, No. 2, March-April 2004, 174-185,
7. Brown, R. B. and Hwang, P. Y. C., *Introduction to Random Signals and Applied Kalman Filtering*, John Wiley and Sons Inc., 3rd edition, 1997.
8. Mehra, R. K., "Approaches to Adaptive Filtering," IEEE Transactions on Automatic Control, Vol. 17, October 1972.
9. Mohamed, A. H. and Schwarz, K. P., "Adaptive Kalman Filtering for INS/GPS," Journal of Geodesy, 73, 1999, pp-193–203.
10. Myers, K. A. and Tapley, B. D., "Adaptive Sequential Estimation with Unknown Noise Statistics," IEEE Transactions on Automatic Control, Vol. 21, 1976, pp. 520-523.
11. Blanchet, I., Frankignoul C. and Cane, M. A., "A Comparison of Adaptive Kalman Filters for a Tropical Pacific Ocean Model," Monthly Weather Review, American Meteorological Society, Vol. 125, No. 1, Jan., 1997, pp40-58.
12. Julier S. J. and Uhlmann, J. K. "Unscented Filtering and Nonlinear estimation," Proceedings of the IEEE, 92, March 2000, pp. 401-422.
13. Filipski, M. N. and Varatharajoo, R., "Satellite Orbit Estimation Using Earth Magnetic Field Measurements," International Journal of Engineering and Technology, Vol. 3, No. 2, 2006, pp. 263-271.
14. GLONASS COSMOS-2404 Orbit Data, Center for Space Standards and Innovation (CSSI), <http://celestrak.com/NORAD/elements/>
15. Song, Q., Qi, J. and Han, J., "An Adaptive UKF Algorithm and Its Application in Mobile Robot Control," ROBIO '06. IEEE International Conference on Robotics and Biomimetics, Kunming, China, Dec. 2006, pp.1117-1122.